analytical chemistry

pubs.acs.org/ac Article

Ag@Pyc Nanocapsules as Electrochemiluminescence Emitters for an Ultrasensitive Assay of the APE1 Activity

Duo-Duo Chai, Ying Zhuo, Ting-Ting Tu, Hong-Ling Li, Ruo Yuan,* and Sha-Ping Wei*

Cite This: *Anal. Chem.* 2022, 94, 9934−9939 Read Online

ACCESS | Metrics & More | Article Recommendations | Supporting Information

ABSTRACT: Herein, Ag@pyrenecarboxaldehyde nanocapsules (Ag@Pyc nanocapsules) as emitters were prepared to construct an ultrasensitive electrochemiluminescence (ECL) biosensor for the detection of the human apurinic/apyrimidinic endonuclease1 (APE1) activity. Ag nanoparticles on the surface of Pyc nanocapsules as coreaction accelerators could significantly promote coreactant peroxydisulfate ($S_2O_8^{2-}$) to generate massive reactive intermediates of sulfate radical anion ($SO_4^{\bullet-}$), which interacted with the Pyc nanocapsules to achieve a strong ECL response. In addition, with the aid of APE1-triggered 3D DNA machine, trace target could be converted into a large number of mimic targets (MTs), which were positively correlated with the activity of APE1. Consequently, the proposed ECL biosensor realized an ultrasensitive detection of APE1 activity with an exceptional linear working range from 5×10^{-10} to 5×10^{-4} U·μL^{-1} and a lower limit of detection of 1.36×10^{-11} U·μL^{-1}. This strategy provided a new approach to construct an efficient ternary system for the detection of biomolecules and early diagnosis of diseases.

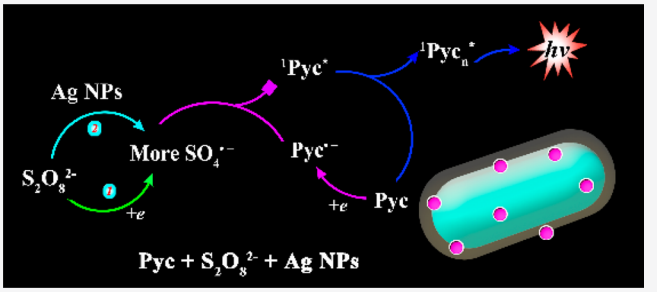

INTRODUCTION

APE1 is an indispensable DNA repair protein in human cells, which performs an integral role in maintaining gene stability and mankind health by recognizing and removing the apurine/pyrimidine (AP) sites during base excision repair.[1−5] Previous reports had shown that abnormal expression of APE1 was closely related to the occurrence of cancer,[3,6−8] so its activity was the key to reflect the condition of the organism. In addition, APE1 as a cancer biomarker is shared by normal and diseased cells, and its expression levels differ only slightly in the early stages.[6,9−11] Currently, the detection of APE1 activity was mainly limited to fluorescent methods.[12−15] However, these fluorescent assays with the inevitable background signal have a limitation in sensitivity and fail to meet the need of trace target detection in early disease diagnosis. Accordingly, it is worth attempting to develop a novel method to detect the activity of low abundance APE1 with high sensitivity and specificity. In this work, an efficient ternary electrochemiluminescence (ECL) biosensor was designed based on Ag@Pyc nanocapsules as the ECL indicator and an APE1-triggered 3D DNA machine as a signal conversion amplifier, which realized ultrasensitive translation of low abundance APE1 activity to signal output.

Herein, an ECL biosensor for sensitively assessing APE1 activity was constructed by the integration of the ECL indicator of a novel self-accelerating Ag@Pyc nanocapsule and an APE1-triggered 3D DNA machine. Noticeably, the simple and well-known silver mirror reaction was employed to synthesize Ag@Pyc nanocapsules for enhancing the ECL efficiency of Pyc nanocapsules as emitters, in which Ag nanoparticles as coreaction accelerators could generate massive reactive intermediates of a sulfate radical anion ($SO_4^{\bullet-}$) to interact with the illuminant for realizing a strong ECL signal (as illustrated in Scheme 1A). Meanwhile, an APE1-triggered 3D DNA machine based on the catalytic hairpin assembly obtained a large number of mimic targets (MTs) with the assistance of Nt.BbvCI, which realized the target conversion and signal amplification (Scheme 1B). In addition, an "on−off−on" ECL platform was constructed (Scheme 1C). First, Ag@Pyc nanocapsules were coated on a bare glassy carbon electrode (GCE) to cross-link with hairpin 3 (H3) by Ag−S bond to obtain an initial ECL signal ("on" state). Then, the ferrocene-labeled DNA strand (DNA-Fc) as a quenching probe bound to H3 to form a "Ω" DNA structure, achieving an extremely low background signal ("off" state). Finally, mimic targets obtained by magnetic separation competitively hybridize with H3 to enable DNA-Fc to leave the electrode for ECL signal recovery ("on" state). In general, the proposed ECL platform realized a low background signal and ultrasensitive assay of trace APE1 activity, which provided a new idea for

Received: May 16, 2022
Accepted: June 17, 2022
Published: June 29, 2022

https://doi.org/10.1021/acs.analchem.2c02122
Anal. Chem. 2022, 94, 9934−9939

Scheme 1. Schematic Depiction of the ECL Biosensor for APE1 Activity Assessment: the Preparation of Ag@Pyc Nanocapsules (A); APE1-Triggered 3D DNA Machine as a Signal Conversion Amplifier (B); the Fabrication of the ECL Biosensor and Signal Response (C)

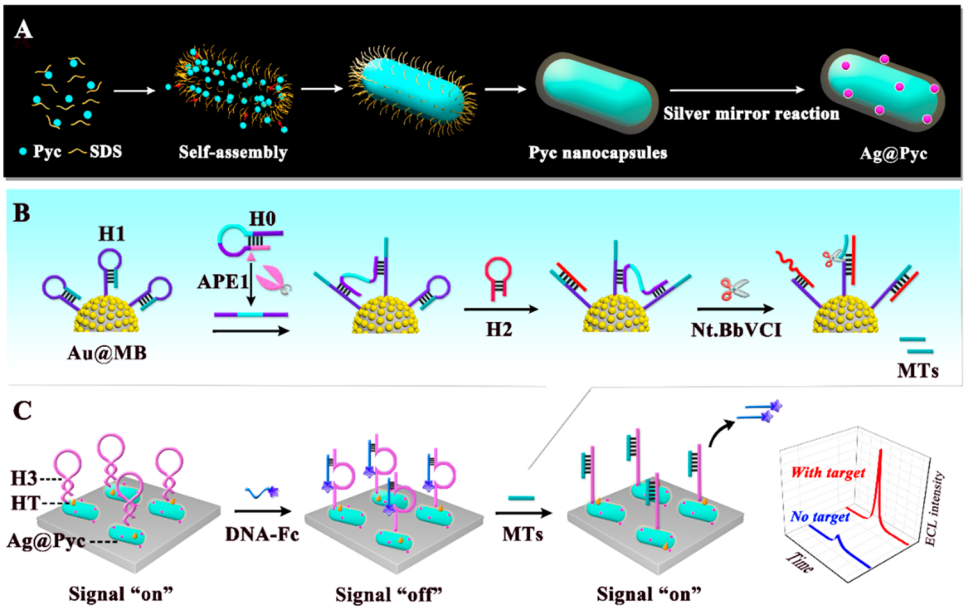

sensitive detection of biomolecules and has a broad application prospect in early disease diagnosis.

EXPERIMENTAL SECTION

Fabrication of the Pyc Nanocapsules. A slightly modified reprecipitation method was used for the synthesis of the Pyc nanocapsules.[16,17] First, 575 μg of 1-pyrenecarboxaldehyde (Pyc) was dispersed in 500 μL of ethanol (EtOH) and then ultrasonicated for 10 min to obtain a homogeneous light yellow solution. Then, the above solution was rapidly injected into 10 mL of the sodium dodecyl sulfate (0.01 M, SDS) solution and reacted at 80 °C for 2 h after vigorous agitation for 10 min, followed by stewing overnight at room temperature. At last, the Pyc nanocapsules were collected after being centrifuged and washed with ultrapure water for several times.

Synthesis of the Ag@Pyc Nanocapsules. The silver−ammonia solution was prepared by slowly dropping 4% $NH_3 \cdot H_2O$ into 1 mL of 0.1 M $AgNO_3$ solution until the formation of a brown precipitate was completely dissolved. Subsequently, the aforementioned solution was mixed with 2 mL of the Pyc nanocapsules at 70 °C for 1 h to obtain Ag@Pyc nanocapsules. It can be observed that the color of the solution changed from light yellow to saffron yellow. After being centrifuged and washed with ultrapure water, Ag@Pyc nanocapsules were dispersed in 4 mL of ultrapure water for later use.

APE1-Triggered 3D DNA Machine as a Signal Conversion Amplifier. First, 500 μL of commercially available NH_2-modified Fe_3O_4 nanoparticles were rinsed with ultrapure water for 3 times, then mixed with the prepared 3 mL of Au nanoparticles (as shown in Supporting Information, 1.3) and were shaken overnight at 4 °C to obtain Au-wrapped Fe_3O_4 nanoparticles (Au@Fe_3O_4 NPs). The Au@Fe_3O_4 NPs were dispersed into 2 mL of PBS after magnetic separation for three times. Then, a mixture of 50 μL of thiol moieties modified hairpin1 (H1, 6 μM) and 50 μL Au@Fe_3O_4 NPs were shaken gently at 4 °C for 12 h to obtain H1/Au@Fe_3O_4 by a Au−S bond. After being magnetically separated and washed three times with PBS, H1/Au@Fe_3O_4 as the 3D DNA machine tracks was successfully prepared and dispersed in 100 μL of PBS and stored at 4 °C for later use.

Subsequently, 10 μL of the target solution containing APE1 and the hairpin 0 (H0, 0.5 μM) and 10 μL of the hairpin 2 (H2, 1 μM) was added into 20 μL of H1/Au@Fe_3O_4 solution to trigger a 3D DNA machine at 37 °C for 2 h. Then, H2/H1/Au@Fe_3O_4 solution was obtained by magnetic separation and washed three times to remove the unreacted residues. Next, the addition of 400 U Nt.BbvCI to the aforementioned solution reacted at 37 °C for 2 h to produce a large number of mimic targets (MTs). After magnetic separation, the supernatant was stored at 4 °C and then used for the proposed biosensor.

Fabrication of the Proposed ECL Biosensor. Initially, the glassy carbon electrode (GCE) was treated with Al_2O_3 powder for polishing and then sonicated alternately with ultrapure water and ethanol for 3 times. Then, 10 μL of the Ag@Pyc nanocapsules solution was coated on the prepared GCE and dried at room temprerature to form Ag@Pyc/GCE. Subsequently, 10 μL of the thiol-functionalized hairpin 3 (H3, 1 μM) was assembled on the modified electrode via Ag−S bond at 4 °C 10 h. Following that, the hexanethiol (HT, 10 μL, 1 mM) was dripped on the resultant electrodes to block the unreacted specific sites. Then, 10 μL of DNA-Fc (1 μM) was immobilized on the electrode to unfold H3 at 37 °C for 2 h. After each step, the modified electrode was rinsed with phosphate buffer saline (PBS, pH 7.4) to remove the reactionless species. The resultant ECL biosensor (DNA-Fc/HT/H3/Ag@Pyc/GCE) stored at 4 °C before use.

Measurement Procedure. Briefly, different concentrations of APE1 triggered the 3D DNA machine as a signal conversion amplifier to generate large amounts of MTs. After that, 10 μL of supernatant containing MTs was dripped on DNA-Fc/HT/H3/Ag@Pyc/GCE and incubated at 37 °C for 2 h. After the prepared electrode was gently washed with PBS to

https://doi.org/10.1021/acs.analchem.2c02122
Anal. Chem. 2022, 94, 9934−9939

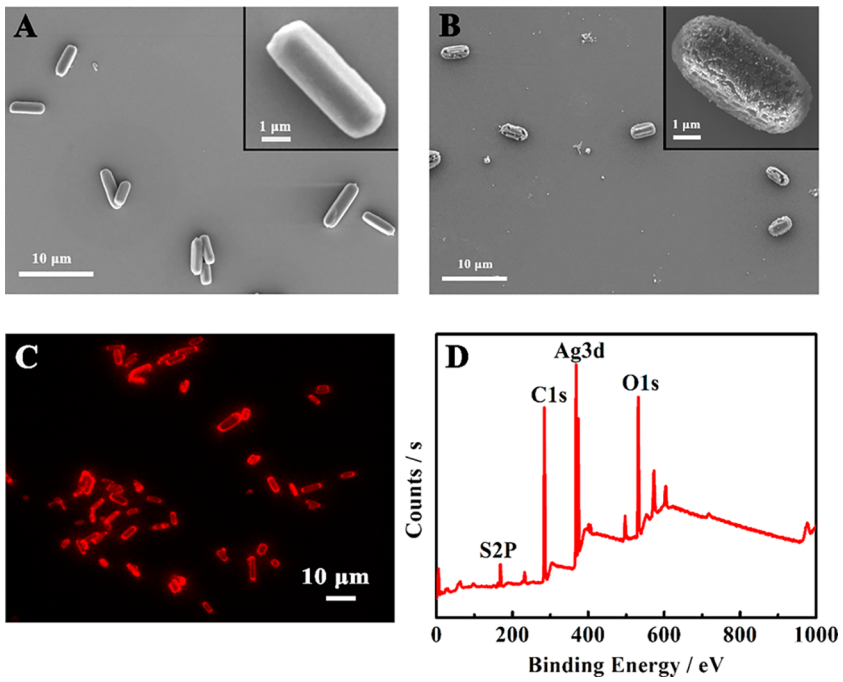

Figure 1. SEM images of (A) Pyc nanocapsules and (B) Pyc@Ag nanocapsules. (C) Fluorescence microscopic image of Pyc nanocapsules. (D) Full region of Ag@Pyc nanocapsules.

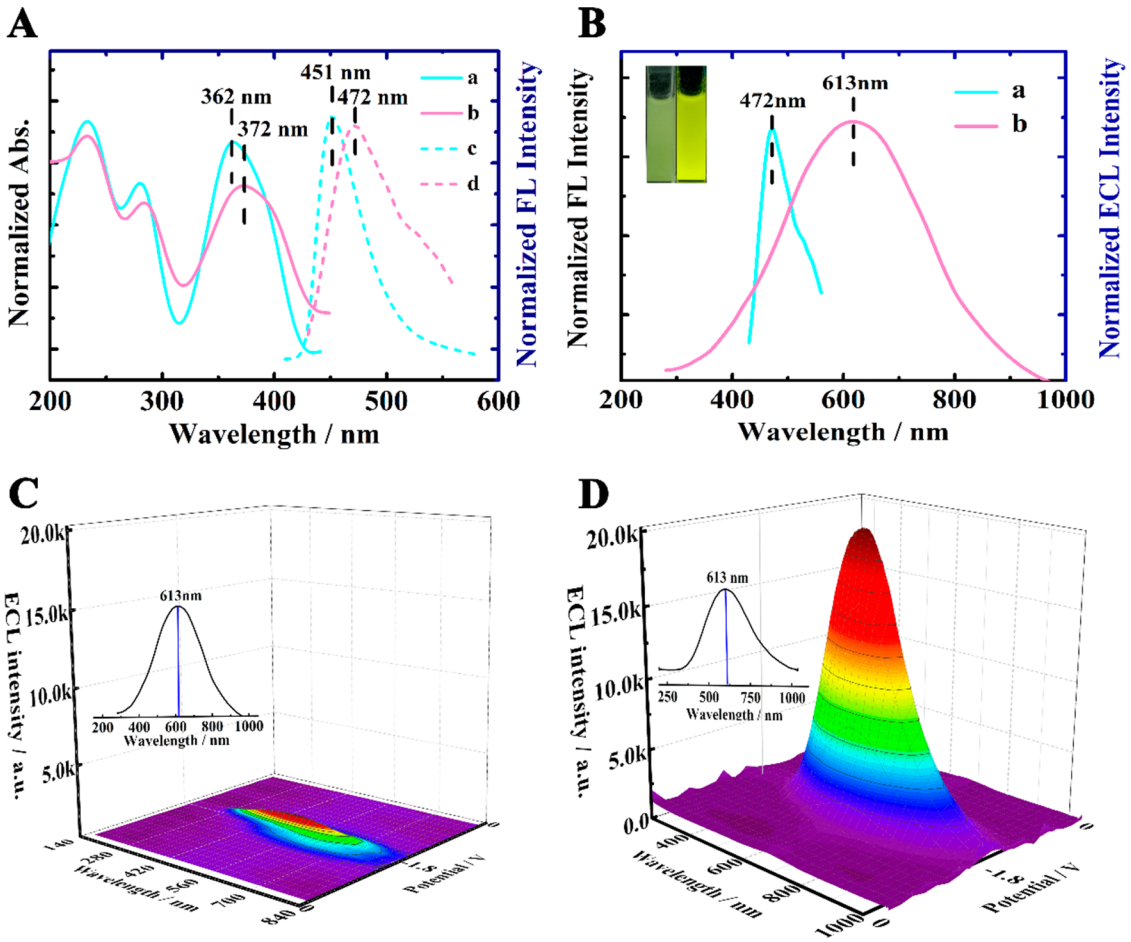

Figure 2. (A) UV−vis spectrum of (a) Pyc in ethanol, (b) Pyc nanocapsules in aqueous solution, the FL emission spectrum of (c) Pyc dissolved in ethanol and (d) Pyc nanocapsules in aqueous solution. (B) FL spectra and the maximum ECL spectra of Pyc nanocapsules. Inset of (B) images of Pyc nanocapsules under the visible daylight (left) and UV light (right). (C) 3D ECL spectrum of Pyc nanocapsules and (D) Ag@Pyc nanocapsules.

https://doi.org/10.1021/acs.analchem.2c02122
Anal. Chem. 2022, 94, 9934−9939

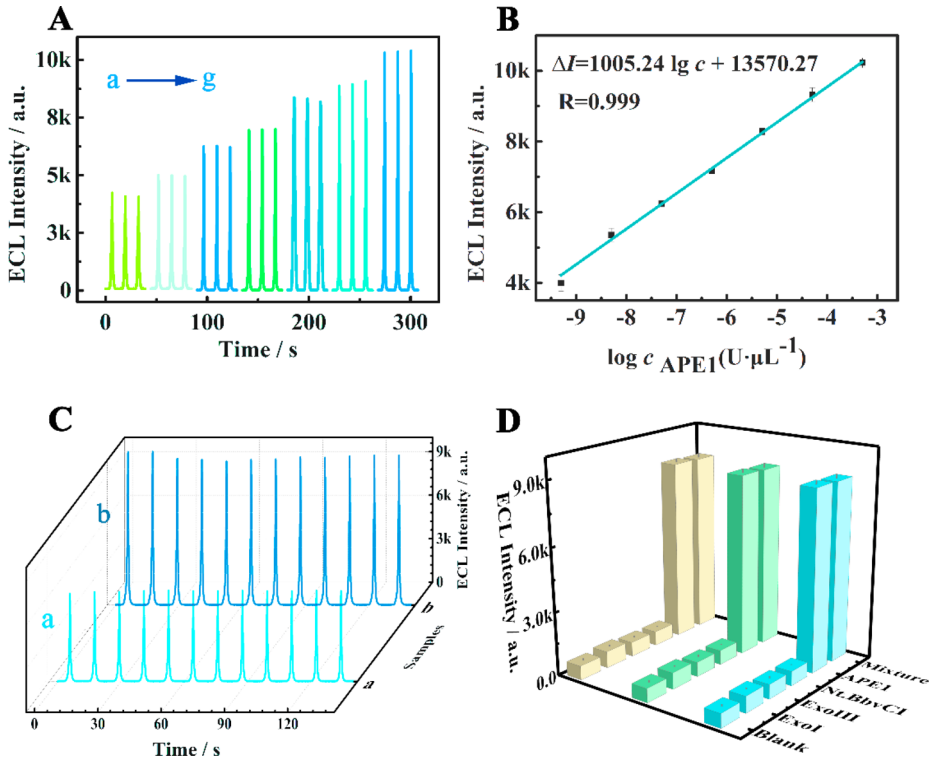

Figure 3. (A) ECL responses of the proposed biosensor with different concentrations of APE1 (a–g): 5×10^{-10}, 5×10^{-9}, 5×10^{-8}, 5×10^{-7}, 5×10^{-6}, 5×10^{-5}, and 5×10^{-4} U·μL^{-1}. (B) The calibration plot of the ECL biosensor for assessing human APE1 activity. Error bars, SD, $n = 3$. (C) Stability of the proposed biosensor with 5×10^{-8} U·μL^{-1} (a) and 5×10^{-4} U·μL^{-1} (b) APE1, respectively. (D) Selectivity of the proposed biosensor: blank, 5×10^{-4} U·μL^{-1} Exo I, 5×10^{-4} U·μL^{-1} Exo III, 5×10^{-4} U·μL^{-1} Nt.BbvCI, 5×10^{-6} U·μL^{-1} APE1, and a mixture.

remove released DNA-Fc and needless products. The ECL signal of the prepared electrode was obtained in 2 mL of $K_2S_2O_8$ (10 mM, pH 7.4) solution by MPI-E ECL analyzer in the potential range of −1.8 to 0 V, with a photomultiplier tube (PMT) voltage set at 700 V.

RESULTS AND DISCUSSION

Morphology and Structure Characterization of Pyc Nanocapsules and Ag@Pyc Nanocapsules. The morphologies of the prepared Pyc nanocapsules and Ag@Pyc nanocapsules were studied by scanning electron microscopy (SEM) in Figure 1A,B. It was obviously exhibited that the obtained nanomaterials were capsule-like structures of 4 ± 1 μm side length. Compared to Pyc nanocapsules, the Ag@Pyc nanocapsules surface was rougher due to Ag nanoparticles coated on the Pyc nanocapsules. As expected, the fluorescence image in Figure 1C showed that the morphology and size of Pyc nanocapsules were approximately in accordance with the SEM image. As illustrated in Figure 1D, the Ag 3d peak, O 1s peak, C 1s peak, and S 2p peak in X-ray photoelectron spectroscopy (XPS) further confirmed the chemical content of the Ag@Pyc nanocapsules. Besides, the Ag 3d peaks at 368.3 and 374.5 eV could be observed, which verified the existence of Ag nanoparticles on the Pyc nanocapsules (as shown in Figure S2 of the Supporting Information, 2.2).[18] Also, the peaks at 531.9, 283.5, and 168 eV were O 1s, C 1s, and S 2p, respectively, indicating the presence of Pyc and SDS.

Optical Properties of the Nanocapsules. The optical properties of the nanocapsules were investigated by UV–vis, fluorescence, and ECL spectra. As presented in Figure 2A, the monodisperse Pyc dissolved in ethanol was observed by UV–vis absorption spectroscopy with characteristic peaks at 236, 278, and 362 nm, respectively (curve a). Meanwhile, the UV peaks of Pyc nanocapsules in aqueous solution changed from 362 to 372 nm (curve b). Similarly, the fluorescence emission peaks of the monodisperse Pyc (curve c) and the Pyc nanocapsules (curve d) were located at 451 and 472 nm, respectively, occurred with a 21 nm red shift. As exhibited in Figure 2B, the maximum ECL emission of Pyc nanocapsules had a significant red shift with 141 nm compared to the fluorescence emission. These red-shift phenomena indicated the aggregation of Pyc molecules with the formation of strong π–π stacking interactions.[19,20] Meanwhile, the solution of Pyc nanocapsules appeared light yellow when placed in visible light and bright yellow under UV light (the inset of Figure 2B). Additionally, the three-dimensional (3D) ECL spectra was used to explore the ECL properties of Pyc nanocapsules and Ag@Pyc nanocapsules. As depicted in Figure 2C,D, the same maximum ECL emission of Pyc nanocapsules and Ag@Pyc nanocapsules can be observed at 613 nm, verifying that the emission of Pyc in the excited state. Noticeably, compared with the ECL response of Pyc nanocapsules (1039 au), the ECL response of the Ag@Pyc nanocapsules (16975 au) was amplified by 16.3-fold due to the fact that Ag nanoparticles could be served as coreaction accelerators to enhance the ECL efficiency.

Evaluation of the Performance of the Proposed Biosensor. To estimate the performance of the fabricated ECL biosensor, the ECL response of different concentrations of APE1 was measured under the optimum reaction conditions (the process of optimizing the conditions were described in Figure S7). As presented in Figure 3A, the ECL responses increased gradually with the enhancement of APE1 concentration in the range of $5 \times 10^{-10} \sim 5 \times 10^{-4}$ U·μL^{-1} and

https://doi.org/10.1021/acs.analchem.2c02122
Anal. Chem. 2022, 94, 9934–9939

presented a favorable linear relationship with the logarithm of APE1 concentration. Noticeably, the linear regression equation was $I = 1005.24 \lg c + 13570.27$ with a detection limit of 1.36×10^{-11} U·μL^{-1} ($S/N = 3$) in Figure 3B.

The stability and selectivity were regarded as two crucial indicators to assess the performance of ECL biosensors. As depicted in Figure 3C, 5×10^{-8} U·μL^{-1} (a) and 5×10^{-4} U·μL^{-1} (b) APE1 were used to determine the stability of the proposed biosensor. It can be noticed that the ECL response of this biosensor remained almost stable over 12 consecutive curves and the relative standard deviations (RSD) were 0.850% (a) and 1.711% (b), indicating that the ECL platform equipped with an outstanding stability. Besides, the biosensor selectivity was assessed by measuring different enzymes, such as Exo I, Exo III, and Nt.BbvCI. Moreover, the proposed biosensor had high-intense ECL signal only in the addition of APE1, while the other enzymes exhibited ECL response almost similar to the background signal in Figure 3D. It implied that the ECL biosensor was highly specific for the detection of APE1.

Application of the ECL Biosensor in Actual Samples. In order to test the applicability of the proposed ECL biosensor for the detection of real samples, in this work, the retrieving rate of this biosensor was investigated by using the standard addition method. APE1 activity was measured by adding different concentrations of target solution to human serum (diluted 50-fold in PBS). The recovery concentrations were calculated according to the previously calibrated curve (Figure 3B). As displayed in Table 1, the recoveries (95.86−103.21%) and RSDs (0.725−1.22%) of APE1 were within the permissible range, which implied the potential of this ECL biosensor for monitoring APE1 in the practical sample analysis.

Table 1. Determination of APE1 in Serum Samples

sample number	added (U·μL^{-1})	found (U·μL^{-1})	recovery (%)	RSD (%)
1	5.000×10^{-4}	5.0776×10^{-4}	101.55	0.725
2	5.000×10^{-6}	4.7930×10^{-6}	95.86	0.738
3	5.000×10^{-7}	5.1603×10^{-7}	103.21	1.22

CONCLUSIONS

In summary, we constructed an efficient ternary ECL biosensor for assessing human APE1 activity with high recognition specificity and amplification efficiency, which was attributed to the integration of the ECL indicator of a novel self-accelerating Ag@Pyc nanocapsule and an APE1-triggered 3D DNA machine. Specifically, Ag nanoparticles as coreaction accelerators were uniformly attached to the surface of Pyc nanocapsules via a silver mirror reaction to enhance ECL efficiency. In addition, the 3D DNA machine accumulated signals during the walking process, and it output a large number of mimic targets with the assistance of Nt.BbvCI, which achieved direct translation of APE1 activity to ECL signal output with a lower limit of detection of 1.36×10^{-11} U·μL^{-1}. The proposed ECL biosensor provided a new pathway to assess APE1 activity and had great potential for the application in the evaluation of biomolecules and the early diagnosis of cancer.

ASSOCIATED CONTENT

Supporting Information

The Supporting Information is available free of charge at https://pubs.acs.org/doi/10.1021/acs.analchem.2c02122.

Materials and reagents, instrument, preparation of Au nanoparticles, TEM characterization of Au nanoparticles, XPS spectra of the different elements region, feasibility analysis of the APE1-triggered 3D DNA machine, ECL enhancement mechanism of Ag@Pyc nanocapsules, ECL spectra of the ECL ternary system, characterization of the ECL biosensor, optimization of the reaction condition, the calculation procedure of the LOD, and comparison of different methods for APE1 detection (PDF)

AUTHOR INFORMATION

Corresponding Authors

Ruo Yuan − *Key Laboratory of Luminescence Analysis and Molecular Sensing (Southwest University), Ministry of Education, College of Chemistry and Chemical Engineering, Southwest University, Chongqing 400715, People's Republic of China*; orcid.org/0000-0003-3664-6236; Phone: +86-23-68252277; Email: yuanruo@swu.edu.cn; Fax: +86-23-68253172

Sha-Ping Wei − *Key Laboratory of Luminescence Analysis and Molecular Sensing (Southwest University), Ministry of Education, College of Chemistry and Chemical Engineering, Southwest University, Chongqing 400715, People's Republic of China*; Email: shapingw@swu.edu.cn

Authors

Duo-Duo Chai − *Key Laboratory of Luminescence Analysis and Molecular Sensing (Southwest University), Ministry of Education, College of Chemistry and Chemical Engineering, Southwest University, Chongqing 400715, People's Republic of China*

Ying Zhuo − *Key Laboratory of Luminescence Analysis and Molecular Sensing (Southwest University), Ministry of Education, College of Chemistry and Chemical Engineering, Southwest University, Chongqing 400715, People's Republic of China*; orcid.org/0000-0002-4491-1186

Ting-Ting Tu − *Key Laboratory of Luminescence Analysis and Molecular Sensing (Southwest University), Ministry of Education, College of Chemistry and Chemical Engineering, Southwest University, Chongqing 400715, People's Republic of China*

Hong-Ling Li − *Key Laboratory of Luminescence Analysis and Molecular Sensing (Southwest University), Ministry of Education, College of Chemistry and Chemical Engineering, Southwest University, Chongqing 400715, People's Republic of China*

Complete contact information is available at: https://pubs.acs.org/10.1021/acs.analchem.2c02122

Notes

The authors declare no competing financial interest.

ACKNOWLEDGMENTS

This work was financially supported by the National Natural Science Foundation (NNSF) of China (22174113, 22176153, and 21974108).

REFERENCES

(1) Antoniali, G.; Serra, F.; Lirussi, L.; Tanaka, M.; D'Ambrosio, C.; Zhang, S.; Radovic, S.; Dalla, E.; Ciani, Y.; Scaloni, A.; Li, M.; Piazza, S.; Tell, G. *Nat. Commun.* **2017**, *8*, 797.
(2) Aboelnga, M. M.; Wetmore, S. D. *J. Am. Chem. Soc.* **2019**, *141*, 8646−8656.
(3) Zhai, J. Q.; Zhao, M. H.; Cao, X. J.; Li, M. Y.; Zhao, M. P. *J. Am. Chem. Soc.* **2018**, *140*, 16925−16928.
(4) Chen, H. Q.; Yao, L. H.; Brown, C.; Rizzo, C. J.; Turesky, R. J. *Anal. Chem.* **2019**, *91*, 7403−7410.
(5) Whitaker, A. M.; Freudenthal, B. D. *DNA Repair* **2018**, *71*, 93−100.
(6) Zhang, Y.; Hua, R. N.; Zhang, C. Y. *Anal. Chem.* **2020**, *92*, 4700−4706.
(7) Housh, K.; Jha, J. S.; Yang, Z.; Haldar, T.; Johnson, K. M.; Yin, J.; Wang, Y.; Gates, K. S. *J. Am. Chem. Soc.* **2021**, *143*, 15344−15357.
(8) Caston, R. A.; Gampala, S.; Armstrong, L.; Messmann, R. A.; Fishel, M. L.; Kelley, M. R. *Drug Discovery Today* **2021**, *26*, 218−228.
(9) Zhai, J. Q.; Liu, Y. B.; Huang, S.; Fang, S. M.; Zhao, M. P. *Nucleic Acids Res.* **2017**, *45*, e45.
(10) Jiang, Y.; Kong, X. J.; Jiang, Y. X. L.; Zhao, W. J.; Zhou, H. M.; Zhang, S. S. *ACS Appl. Bio Mater.* **2020**, *3*, 8507−8514.
(11) Shao, Y. L.; Zhao, J.; Yuan, J. Y.; Zhao, Y. L.; Li, L. L. *Angew. Chem., Int. Ed.* **2021**, *60*, 8923−8931.
(12) Fang, S. M.; Chen, L.; Zhao, M. P. *Anal. Chem.* **2015**, *87*, 11952−11956.
(13) Zhang, Y.; Deng, Y. N.; Wang, C. S.; Li, L. D.; Xu, L. D.; Yu, Y. J.; Su, X. *Chem. Sci.* **2019**, *10*, 5959−5966.
(14) Hu, Y. Q.; Zhang, Z.; Ye, W. C.; Zhang, W.; Hu, M. H.; Yuan, W. Q.; Wang, H. B.; Xiao, X. J.; Wu, T. B. *Sens. Actuators B Chem.* **2021**, *330*, 129332.
(15) Li, G. L.; Li, J. J.; Li, Q. *Nanoscale* **2019**, *11*, 20456−20460.
(16) Sun, S. B.; Yuan, D.; Xu, Y.; Wang, A. F.; Deng, Z. T. *ACS Nano* **2016**, *10*, 3648−57.
(17) Jiang, M. H.; Li, S. K.; Zhong, X.; Liang, W. B.; Chai, Y. Q.; Zhuo, Y.; Yuan, R. *Anal. Chem.* **2019**, *91*, 3710−3716.
(18) Zhou, Y. Z.; Yang, J.; He, T. T.; Shi, H. F.; Cheng, X. N.; Lu, Y. X. *Small* **2013**, *9*, 3445−54.
(19) Figueira-Duarte, T. M.; Mullen, K. *Chem. Rev.* **2011**, *111*, 7260−7314.
(20) Werner, T. C.; Chang, J.; Hercules, D. M. *J. Am. Chem. Soc.* **1970**, *92*, 5560−5565.

https://doi.org/10.1021/acs.analchem.2c02122
Anal. Chem. 2022, 94, 9934−9939